

# NANO • MICRO small

# Temporal Sampling of Enzymes from Live Cells by Localized Electroporation and Quantification of Activity by SAMDI Mass Spectrometry

Prithvijit Mukherjee, Eric J. Berns, Cesar A. Patino, Elamar Hakim Mouly, Lingqian Chang, S. Shiva P. Nathamgari, John A. Kessler, Milan Mrksich,\* and Horacio D. Espinosa\*

Measuring changes in enzymatic activity over time from small numbers of cells remains a significant technical challenge. In this work, a method for sampling the cytoplasm of cells is introduced to extract enzymes and measure their activity at multiple time points. A microfluidic device, termed the live cell analysis device (LCAD), is designed, where cells are cultured in microwell arrays fabricated on polymer membranes containing nanochannels. Localized electroporation of the cells opens transient pores in the cell membrane at the interface with the nanochannels, enabling extraction of enzymes into nanoliter-volume chambers. In the extraction chambers, the enzymes modify immobilized substrates, and their activity is quantified by self-assembled monolayers for matrix-assisted laser desorption/ionization (SAMDI) mass spectrometry. By employing the LCAD-SAMDI platform, protein delivery into cells is demonstrated. Next, it is shown that enzymes can be extracted, and their activity measured without a loss in viability. Lastly, cells are sampled at multiple time points to study changes in phosphatase activity in response to oxidation by hydrogen peroxide. With this unique sampling device and label-free assay format, the LCAD with SAMDI enables a powerful new method for monitoring the dynamics of cellular activity from small populations of cells.

## 1. Introduction

Enzymes represent an important class of proteins that carry out a diverse set of functions within cells, and the ability to measure their activity is critical for the study of cell and molecular biology. For example, the protein tyrosine phosphatases (PTPs), a set of enzymes that act in opposition to protein tyrosine kinases, play critical roles in many key biological processes and in oncogenesis.<sup>[1]</sup> Many PTPs, including PTEN, PTP1B, RPTP $\alpha$ , and the PRLs change expression or activity levels in various cancers, and some, such as SHP2, are oncogenes themselves.<sup>[2]</sup>

Methods for quantifying enzymatic activities from cell samples frequently require cell lysis, a destructive process that prevents the acquisition of measurements from multiple time points for a given sample. As a result, tracking dynamic cell behavior in response to external and internal regulatory factors becomes challenging.

P. Mukherjee, C. A. Patino, Dr. L. Chang, S. S. P. Nathamgari, Prof. H. D. Espinosa  
Department of Mechanical Engineering  
Northwestern University  
Evanston, IL 60208, USA  
E-mail: espinosa@northwestern.edu


P. Mukherjee, S. S. P. Nathamgari, Prof. H. D. Espinosa  
Theoretical and Applied Mechanics Program  
Northwestern University  
Evanston, IL 60208, USA

Prof. E. J. Berns, Prof. M. Mrksich  
Department of Biomedical Engineering  
Northwestern University  
Evanston, IL 60208, USA  
E-mail: milan.mrksich@northwestern.edu

E. Hakim Mouly, Prof. M. Mrksich  
Department of Chemistry  
Northwestern University  
Evanston, IL 60208, USA

Prof. J. A. Kessler  
Department of Neurology  
Northwestern University Feinberg School of Medicine  
Chicago, IL 60611, USA

Prof. M. Mrksich  
Department of Cell and Development Biology  
Northwestern University Feinberg School of Medicine  
Chicago, IL 60611, USA

 The ORCID identification number(s) for the author(s) of this article can be found under <https://doi.org/10.1002/smll.202000584>.

DOI: 10.1002/smll.202000584



Moreover, in many cases, cell populations of interest are available in limited quantities, for example, cells from a biopsy or a rare subpopulation of cells, making many traditional enzymatic assay formats unsuitable for investigating their activity. Thus, there is a need to develop techniques that can nondestructively sample enzymes from small populations of living cells and quantify their activity at multiple time-points. Recent methods for nondestructive sampling have used nanopipettes and hollow atomic force microscope (AFM) tips to extract and analyze cytosolic and nuclear content from individual cells.<sup>[3,4]</sup> However, due to the serial nature of these systems, few cells can be addressed at a time, which limits the throughput. To overcome these limitations, we investigated a method that pairs a recently developed method for nondestructive cellular delivery and extraction, called localized electroporation,<sup>[5–9]</sup> with a versatile, label-free platform for quantifying enzymatic activities in complex mixtures, called self-assembled monolayers for matrix-assisted laser desorption/ionization (SAMDI) mass spectrometry.<sup>[10]</sup>

Bulk electroporation is an extensively used technology, for delivering exogenous molecules such as proteins and nucleic acids into cells and tissues by temporarily disrupting the cell membrane with strong electric fields.<sup>[11,12]</sup> Localized electroporation is an emerging method wherein the applied electric field is confined to a fraction of the plasma membrane by nanostructures such as nanochannels, nanopores or nanostraws.<sup>[5,13–16]</sup> This provides certain advantages over bulk electroporation such as high cell viability, electroporation uniformity and excellent dosage control. Localized electroporation is effective in delivering a wide range of cargos such as small molecule dyes, proteins, RNA, plasmid DNA and other molecular probes, into a variety of cell types including primary cells.<sup>[17,18]</sup> Recently, it has also been utilized for cellular extraction and analysis of cytoplasmic proteins and mRNA, while keeping the cells viable.<sup>[6,7,19]</sup> In this work, we use localized electroporation in microfluidic devices to extract enzymes for activity measurement with SAMDI.

SAMDI uses monolayers on gold-coated slides or plates to present substrates to enzymes.<sup>[10,20]</sup> The monolayers are composed of alkanethiolates; 90% of these are terminated with tri(ethylene glycol) to prevent nonspecific adsorption of proteins to the monolayer and 10% of the alkanethiolates are terminated with a maleimide group, enabling immobilization of substrates with a thiol group. After exposure to a solution containing enzymes, immobilized substrates are modified by the enzymes. A matrix is then applied to the monolayers and matrix-assisted laser desorption/ionization (MALDI) mass spectrometry is performed, where the laser desorbs alkanethiolates covalently attached to the substrates and products. For enzymatic activities that produce a mass change in the substrate, SAMDI quantifies enzymatic activity by measuring the relative amounts of substrate and product observed in the mass spectrum. SAMDI can be easily adapted to measure activities of a broad range of enzyme subclasses, including kinases, phosphatases, deacetylases, glycosyltransferases, caspases, proteases, and others.<sup>[21–26]</sup> SAMDI does not require significant alteration of substrates with labels, which can modify enzymatic activity and can require extensive development.<sup>[27,28]</sup> For example, fluorescent probes can alter enzymatic activity measurements by more than 50-fold.<sup>[27,28]</sup> For this investigation, we

use SAMDI to measure the activities of PTPs, which remove a phosphate group from the phenol on the tyrosine side chain, resulting in a  $-80$  Da shift in the mass.<sup>[22]</sup>

Herein, we introduce the live cell analysis device (LCAD) with SAMDI—a nondestructive method for sampling enzymes and measuring their activity from small numbers of cells. The LCAD with SAMDI uses a microfluidic device format to isolate small groups of cells, from which PTPs are extracted through membranes with nanochannels via localized electroporation, followed by measurement of their activity with SAMDI. We show that cells remain viable after the electroporation procedure and can be sampled at multiple time points, enabling measurement of enzymatic activities from small numbers of cells over time.

## 2. Results

### 2.1. LCAD Design

The design of the LCAD enables the extraction and analysis of cytosolic contents from live cells while preserving their viability. The LCAD is a multi-layered microfluidic device (**Figure 1A**) that allows for cell seeding via microfluidic channels (layer 2) and long-term culture of adherent cells in isolated microwells (layer 3). A thin gold layer between the microfluidic channels and microwells enhances electrical conductivity and minimizes electric field losses in the channels. The cells adhere to a fibronectin-coated polycarbonate (PC) membrane (layer 4) containing 200 nm diameter nanochannels (density of  $5 \times 10^8$  pores  $\text{cm}^{-2}$ ), that span the membrane, enabling the extraction of cytosolic molecules into the bottom microchambers (layer 5, extraction chambers) via localized electroporation. This nanochannel density results in  $\approx 15\%$  of the attached cell membrane interfacing with the nanochannels. A pulsed electric field is applied to the cells via removable electrode layers: the indium titanium oxide- (ITO) coated slide on the top (layer 1) and the conductive SAMDI slide on the bottom (layer 6). This leads to formation of transient pores in the cell membrane areas collocated with the nanochannels, through which the cytosolic milieu is transported into extraction chambers that interface with the SAMDI slide. The SAMDI slide is an ITO coated slide with circular gold patterns that serves the dual purpose of acting as an electrode and providing a surface for immobilization of the substrates for enzymatic reactions. The extraction chambers provide small reaction volumes (4.8 nL) for the extracted intracellular enzymes to act on the substrates immobilized on the SAMDI slide. The enzymatic activity is then quantified using SAMDI mass spectrometry (**Figure 1B**).

### 2.2. Device Fabrication

The LCAD is designed to perform several functions in one device and, as a result, requires surface chemistry modification, precise alignment, and bonding of multiple layers composed of different materials (**Figure 2A**). Fabrication comprises three steps: i) soft lithography of polydimethylsiloxane (PDMS) microchannels and microwells, ii) gold (Au) deposition of

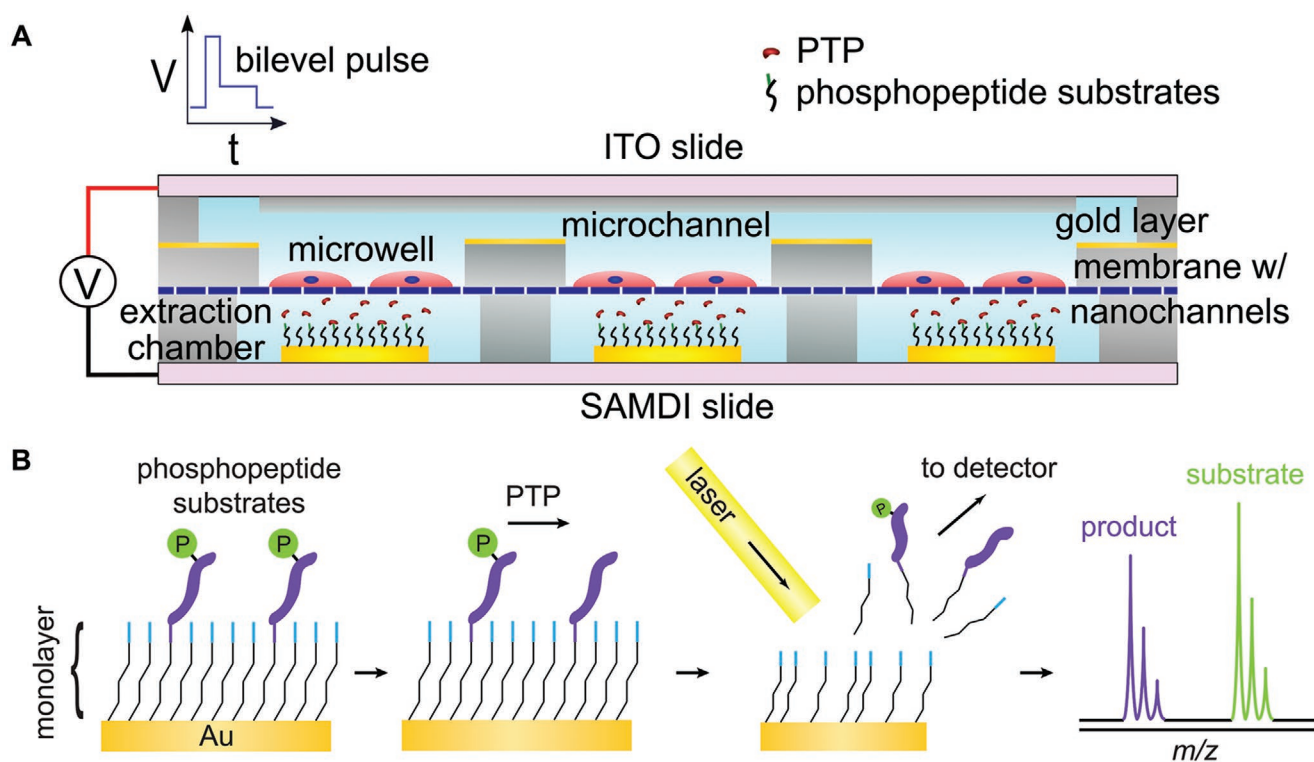


**Figure 1.** The LCAD with SAMDI. A) A schematic of the side view of the LCAD architecture. Cells are loaded into microchannels and cultured in the microwells. Electric pulses open transient pores and extract enzymes through nanochannels into the extraction chamber, where they modify immobilized substrates on the gold-coated SAMDI slide. B) The SAMDI workflow (left to right): peptides are immobilized on a monolayer on the SAMDI slide; extracted PTPs dephosphorylate the substrate; the MALDI laser desorbs the immobilized substrates and products; mass spectra are analyzed to quantify enzyme activity.

embedded electrodes, and iii) alignment and bonding of the multiple layers using surface chemistry treatments. In the first step, microchannels are prepared using standard soft lithography techniques, with additional processing steps required to make the through-holes in the microwell layers.<sup>[29]</sup> In order

to apply a uniform electric field across each of the wells, a 100 nm Au layer is deposited on the top microwell layer. Following fabrication of the layers, the device is assembled as depicted in Figure 2A,B. Two surface chemistry treatments are performed to covalently bond the Au-coated microwells with the PDMS microchannels, and the PC membrane containing nanochannels with the PDMS microwell surfaces. First, the Au microwell surface is treated with a thiol-terminated silane, mercaptopropyl(trimethoxysilane) (MPTMS), and subsequently bonded to the PDMS microchannel layer. After embedding the Au electrodes in the microfluidic device, the two PDMS microwell surfaces are treated with an aminosilane, aminoethylaminopropyl(trimethoxysilane) (AEAPS), and bonded to the PC membrane. The fully assembled device (Figure 2C) was tested for leaks and electrical conductivity prior to experimentation and was found to withstand flow rates ten-fold higher than required for experiments without leakage.

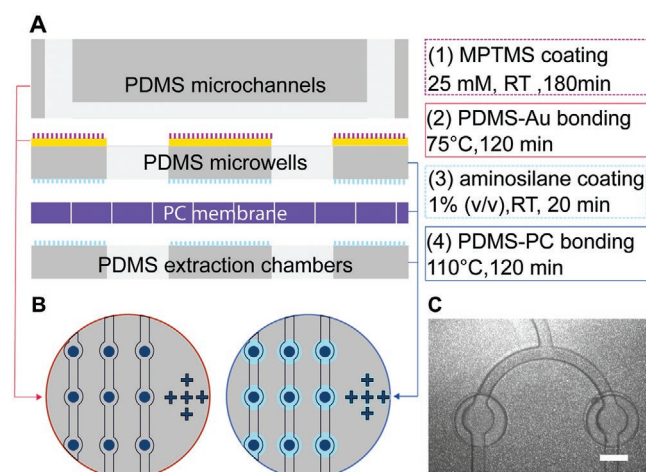


**Figure 2.** The LCAD fabrication and assembly. A) Schematic of multilayer architecture, depiction of chemical modifications, and assembly process. B) Schematic showing alignment of layers. C) Micrograph of channels and wells in an assembled LCAD. Scale bar = 150  $\mu\text{m}$ . (RT = Room Temperature)

### 2.3. Delivery of Fluorescently Labeled Bovine Serum Albumin into Cells

In order to assess the performance of the LCAD platform, we cultured tdTomato-expressing MDA-MB-231 cells—a human, triple negative breast cancer cell line—in the devices. Cells adhered and spread in the microwells, showing typical morphology (Figure 3A). To verify that the electroporation

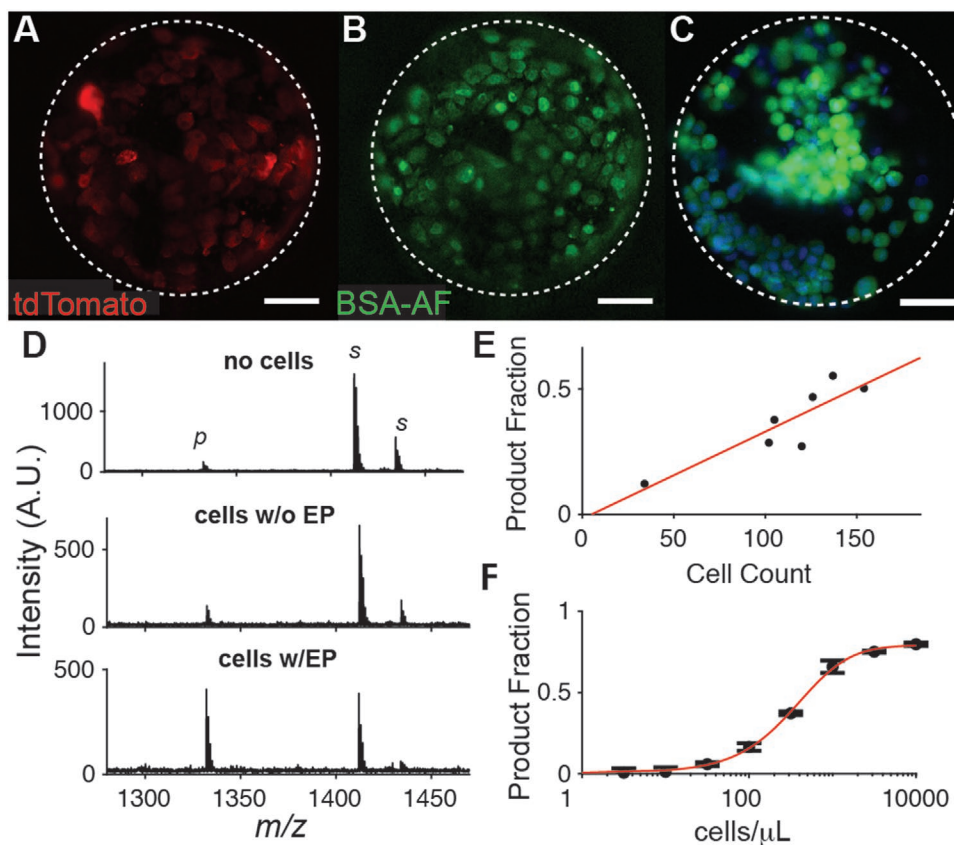


**Figure 3.** Localized electroporation and SAMDI. A) MDA-MB-231 cells expressing tdTomato cultured in an LCAD microwell. All scalebars = 75  $\mu\text{m}$ . B) Delivery of fluorescent BSA (BSA-AF) from the extraction chamber into the cells with localized electroporation. C) A micrograph of cells 24 h after electroporation in an LCAD, labeled with Calcein AM (green) to label viable cells and Hoechst (blue) to label all cells. D) Examples of SAMDI mass spectra for spots corresponding to wells with no cells (top), wells with cells but no electroporation (middle) and wells with cells and electroporation (bottom). p: product peak, s: substrate peak, EP: electroporation. E) The relationship between cell count in microwells in an LCAD device and the observed PTP activity following electroporation. The red line is a linear regression fit of the data ( $R^2 = 0.77$ ). F) PTP activity of lysate (black) and fit (red). Each lysate concentration was reacted on three spots. Error bars represent standard deviation.

protocol enabled transport of proteins across the cell membranes through the nanochannels, we first tested the delivery of Alexa Fluor 488 conjugated bovine serum albumin (BSA) into cultured cells in the LCAD platform. The fluorescent BSA was loaded in the bottom microchambers at a concentration of  $2.5 \text{ mg mL}^{-1}$  in phosphate-buffered saline (PBS) and a train of bi-level electric pulses was applied across the device (see the Experimental Section for details). The cell culture media was replaced by a hypo-osmolar electroporation buffer during the localized electroporation process, which has been previously shown to enhance the efficiency and uniformity of delivery.<sup>[6]</sup> We observed that BSA delivery in the cells cultured on the membranes was uniform and had high efficiency ( $96.6 \pm 1.2\%$ ;  $N = 3$  wells from 1 experiment) (Figure 3B). As a control, we incubated the cells with the hypo-osmolar buffer and fluorescent BSA without the application of the electric pulse and did not observe any significant delivery of BSA (Figure S1, Supporting Information). Consequently, we concluded that the electric field parameters were effective at opening pores in the cell membranes and enabling consistent protein delivery into the cells in the microwells, suggesting that electroporation would also enable extraction of proteins from the cells.

#### 2.4. Sampling Phosphatases from Cells and Measuring Their Activity

Next, we evaluated the ability to extract PTPs from cells and measure their activity with SAMDI. To test this, cells were cultured in the LCAD for  $\approx 36$  h, and then imaged to record the number of cells in each well. Upon localized electroporation, the devices were incubated for 1 h, during which enzymes catalyzed the conversion of immobilized substrates on the monolayers to their dephosphorylated products. SAMDI spectra of controls without cells show adduct peaks corresponding to the mass of the substrate (plus  $\text{H}^+$  and  $\text{Na}^+$  ions) and a very small background peak corresponding to the mass of the dephosphorylated peptide (Figure 3D, top spectrum). This background peak is characteristic of SAMDI spectra of the purified phosphopeptide, likely resulting from minute amounts of dephosphorylated peptides. In contrast, spectra from wells with electroporated cells showed the emergence of a large product peak, indicating successful extraction of functional PTPs into the extraction chamber and dephosphorylation of the immobilized substrates (Figure 3D, bottom spectrum). The devices were loaded with an average of 154 cells per well, and the mean

measurement of PTP activity was  $29 \pm 5\%$  dephosphorylation (above background). Moreover, we observed that the measured PTP activity in an LCAD device was well correlated ( $R^2 = 0.77$ ) with the number of cells in the corresponding microwell (Figure 3E). In order to evaluate the impact of the electroporation procedure on cell viability, we measured viability one day after sampling. We found that cell viability was high following electroporation ( $93.7 \pm 1.5\%$ ;  $N = 3$  wells from 2 experiments) (Figure 3C) and was similar to the viability of cells cultured on membranes which were not electroporated ( $95.1 \pm 0.4\%$ ;  $N = 3$  membranes).

In devices with cells that were not electroporated, a small amount of dephosphorylation ( $4.3 \pm 5\%$ ) was measured (above background), suggesting that even without electroporation, a small but detectable amount of PTP accumulated in the extraction chambers (Figure 3D, middle). However, this level was small compared to that observed following electroporation ( $29 \pm 5\%$ ). This was likely due to cellular exposure to the hypo-osmolar electroporation buffer during the electrode attachment process and incubation period. Incubation in hypo-osmolar buffer is known to apply stress to the cell membranes and has been previously used to temporarily disrupt the plasma membrane for the delivery of molecular cargo.<sup>[30]</sup> One potential solution to minimize osmolarity-related leakage would be to exchange the buffer immediately following electroporation, rather than after the 1 h incubation period. Another solution would be to optimize the LCAD-SAMDI protocol for comparable performance in other buffers.

Next, we compared the amount of phosphatase activity to the amount we observe from cell lysates so that we could approximate the fraction of PTPs extracted with electroporation. We prepared a lysate and measured its activity across a range of concentrations (i.e., cells per microliter of lysis buffer). The measured activities were used to generate a calibration curve (Figure 3F), which was then used to convert measurements of product fractions from the LCAD into the equivalent concentration of cell lysate. Accounting for the volume of the extraction chamber and the number of cells in the microwells, we calculated that  $\approx 1.1\%$  of PTPs, on average, were extracted with these electroporation parameters. With this estimate of the average percentage of extraction, and with the calculation of the cell concentration needed to exceed the limit of detection (LOD), we estimate that the fewest number of cells from which activity would exceed the LOD is 25 cells in these devices, using these electroporation parameters. This matches closely with our measurements; in one device that we loaded with a lower cell density, we observed activity from as few as 21 cells.

## 2.5. Temporal Sampling and Measurement of PTP Activity

We next demonstrated the ability to obtain measurements of PTPs at multiple time points from the same cells. The device is designed to allow for removal of the SAMDI slide after electroporation and incubation. The portion of the device composed of the cell microwells, nanochannel-containing membrane, and extraction chambers can be easily separated from the SAMDI slide and returned to media for cell culture in an incubator.

After the desired lapse of time, a new SAMDI slide can be aligned with the microwells and clamped to the device for another round of electroporation (Figure 4A).

With this approach, we sampled cells in the LCAD on two consecutive days, imaging the cells before each electroporation to account for the number of cells per well (Figure 4B). We observed a 19% increase in average phosphatase activity from Day 2 to Day 3 (from 31% to 37% dephosphorylation). Average cell number per well also increased 13%, due to cell proliferation. Accounting for the number of cells per well, the average activity per cell increased 7.2% and was not significantly different from Day 2 to Day 3 (Figure 4C). These results demonstrate the ability to sample several small populations of cells located in different microwells on multiple days and suggest that the levels of extraction and measured activity are similar from one electroporation to the next.

## 2.6. Sampling and Measurement before and after Treatment with Hydrogen Peroxide

The device is designed to accommodate experimental treatment of the cultured cells, with delivery of reagents to the cells via the microfluidic channels. Measurement of the activity before treatment acts as a baseline readout of activity to which post-treatment measurements from the same populations of cells can be compared. To demonstrate this capability, we used the device to measure the effects of hydrogen peroxide ( $\text{H}_2\text{O}_2$ ), a reactive oxygen species involved in PTP regulation,<sup>[31]</sup> on PTP activity at multiple timepoints. PTP active sites contain a catalytic cysteine residue that can be reversibly oxidized to sulfenic acid or related states, or irreversibly oxidized to sulfinic acid or sulfonic acid derivatives and are inactive in their oxidized states.<sup>[32]</sup>

To this end, we first obtained a baseline measurement of phosphatase activity from cells in a device using the established electroporation sampling procedure. Upon loading the microchannels and treating the cells with  $2 \times 10^{-3} \text{ M}$   $\text{H}_2\text{O}_2$ , a second sampling was performed. For wells with greater than 20% activity at the first time point, we observed a reduction in average PTP activity per cell of 55% ( $P = 0.005$ ) following  $\text{H}_2\text{O}_2$  treatment (Figure 5C). Such reduction is in good agreement with reports of oxidation and inactivation of PTPs by  $\text{H}_2\text{O}_2$ .<sup>[31,33]</sup> To ensure that the reduction in activity was not due to cell death, we measured viability of cells treated with  $2 \times 10^{-3} \text{ M}$   $\text{H}_2\text{O}_2$  and observed high levels of viability (99.7%). As a control, we measured the PTP activity in a device that was not treated with  $\text{H}_2\text{O}_2$ . The average activity measured at the second time point was 23% below the activity at the first time point. This suggests that part of the reduction in activity may be due to the first electroporation.

As previously stated, oxidation by  $\text{H}_2\text{O}_2$  can be reversible or irreversible, resulting in varying degrees of recovery of PTP activity over time.<sup>[31,32]</sup> To assess PTP activity recovery, we cultured the cells for an additional 21 h before sampling them again. Indeed, we observed that the activity had significantly increased ( $P = 0.01$ ) relative to the post-treatment measurement, to a level that was 5% higher than the original mean activity, and was not significantly different than the original measurement ( $P = 0.77$ ) (Figure 5A). When examining the



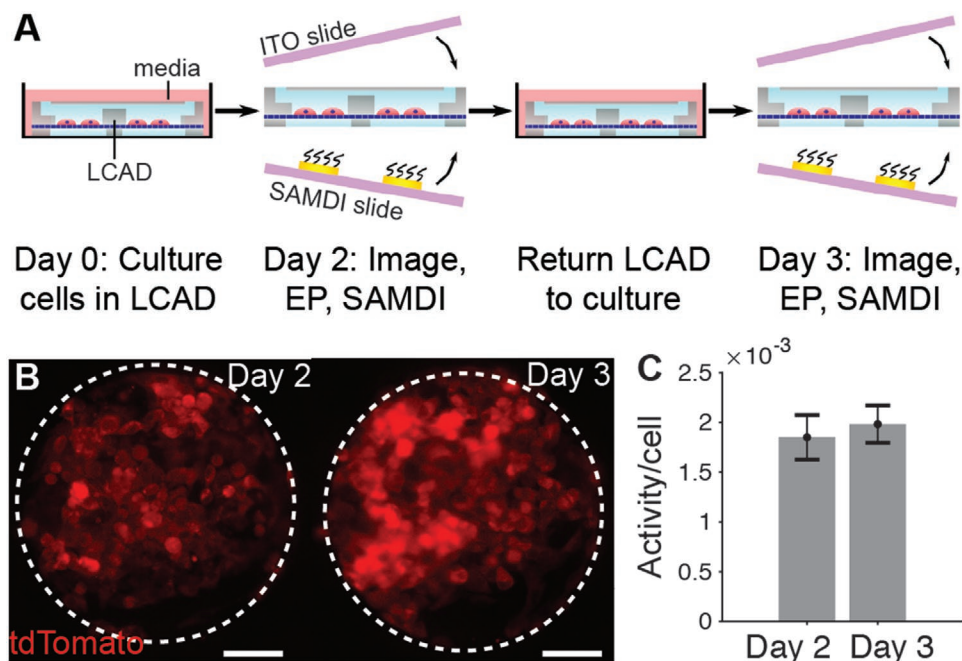


**Figure 4.** Repeated enzyme sampling and activity measurement. A) The process of repeated sampling and measurements in the LCAD with SAMDI. EP: electroporation. B) Fluorescence micrographs of the same representative well in an LCAD, taken on consecutive days immediately before electroporation on that day, showing MDA-MB-231 cells expressing the fluorescent protein tdTomato. Scalebars = 75  $\mu\text{m}$ . C) The average PTP activity per cell, sampled in an LCAD with localized electroporation on consecutive days and measured by SAMDI.  $N = 22$  wells on one LCAD device. Error bars represent the S.E.M.

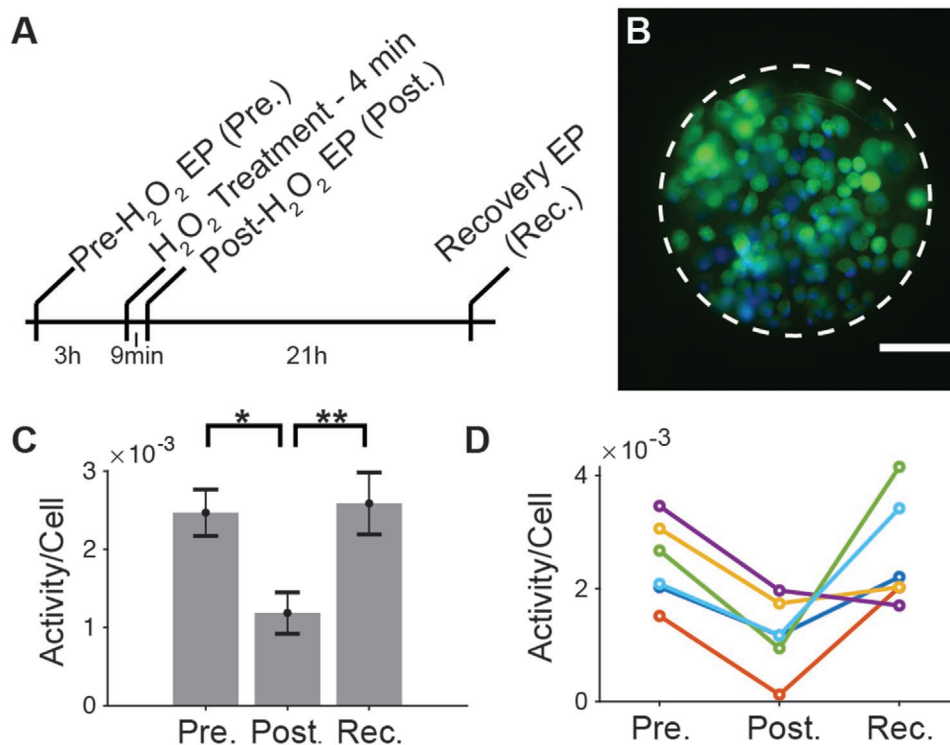


**Figure 5.** Measurement of PTP activity before and after  $\text{H}_2\text{O}_2$  treatment. A) Timeline for sampling with electroporation (EP) and  $\text{H}_2\text{O}_2$  treatment. B) A micrograph of cells 24 h after final sampling, labeled with Hoechst (blue) and calcein AM (green). Scalebar = 100  $\mu\text{m}$ . C) PTP activity per cell measured before (Pre.), shortly after (Post.) and 21 h after  $\text{H}_2\text{O}_2$  treatment.  $N = 6$ . \*  $P = 0.005$ , \*\*  $P = 0.01$ , error bars represent the S.E.M. D) Each line represents the activity per cell of a single well at the three time points.

data for each well at each time point, we observed that all of the wells showed a large reduction in activity after  $\text{H}_2\text{O}_2$  treatment, and most showed at least a partial recovery of activity by the next day (Figure 5D). We measured the viability of the cells 24 h after the final sampling, and again observed high levels of viability (Figure 5B).

### 3. Discussion

In this work, we introduced the LCAD with SAMDI method for longitudinally sampling the cytoplasm of cells in a nondestructive manner and enabling the measurement of changes in enzymatic activity. Several key features were essential for the functionality of these devices. First, localized electroporation at the nanochannels enables the confinement of the electric field to only a fraction of the cell membrane, determined by the density and diameter of the nanochannels in the membrane. This is important for maintaining high cell viability (>90%),<sup>[6]</sup> which was critical to our aim of obtaining multiple measurements from the same cells. The microfluidic format was necessary for isolating small groups of cells and for creating nanoliter-volume reaction chambers to maintain sufficient concentrations of the extracted enzymes for subsequent activity measurements. The complexity of the device, which was composed of six functional layers, was made possible in part from robust bonding between layers, resulting from several chemical surface modifications and materials selections compatible with long-term cell culture. Lastly, the sensitivity, the facile isolation of substrates and products from the complex mixture after the reaction, and the quantitative nature of SAMDI enabled analysis of enzyme activity.

While most of the experiments were performed with cell numbers between 50 and 200 cells per well, we observed PTP activity from as few as 21 cells. The extraction chambers were designed with diameters of 350  $\mu\text{m}$ , but modern MALDI instruments have the capability of acquiring spectra from spots with diameters as small as 10  $\mu\text{m}$ , which indicates that there is potential for reducing the diameter of this chamber. Reduction of the volume of the extraction chamber would enable detection of enzyme activity from fewer cells, and possibly single cells. Further modifications such as exchange of the hypo-osmolar with cell-culture media immediately after the experiment via microfluidic perfusion would minimize osmolarity-induced leakage of cellular material. This would reduce the background and associated experimental variability in the activity measurements leading to improved signal-to-noise ratios and better quantitation of the observed activities. Additional changes, such as optimization of electroporation parameters,<sup>[6]</sup> nanochannel diameter, nanochannel density and careful selection of electroporation buffers, may also aid in obtaining single-cell measurements of enzyme activities. Design improvements that enhance sensitivity will expand the utility of this assay to enzymes with lower copy numbers and slower kinetics, compared to PTPs or other high abundance enzymes. Moreover, in the current study, the LCAD with SAMDI has been demonstrated with adherent cells, where close contact between the cell membrane and nanochannels allows for electroporation to open the localized pores. Although localized electroporation has been utilized for the case of delivery into suspended

cells previously,<sup>[7]</sup> sampling from suspended cells needs to be explored in future research.

In this study, we demonstrated the label-free measurement of PTP activity by SAMDI, but in other work, we have demonstrated the broad utility of the platform for measuring enzyme activities including kinases, deacetylases, glycosyltransferases, caspases, proteases, and others.<sup>[21–26]</sup> By measuring the mass change of the substrate, we do not need to include a fluorogenic, chromogenic, or radioactive label, which can be difficult to develop and can alter the interaction between the substrate and enzyme.<sup>[27,28]</sup> Alteration of the enzyme-probe interaction by fluorescent moieties can lead to results that vary more than 50-fold when compared to unlabeled probes. Measurement of mass also allows for relatively facile translation to a new target, as long as a suitable substrate is known and can be immobilized on a surface through one of a wide range of monolayer surface chemistries.<sup>[10]</sup> PTPs represent an enzyme class encoded by 107 human genes, containing members that are either in cellular membranes or in soluble form.<sup>[34]</sup> From our measurements, we are not able to determine which of the PTPs, or for that matter, which components of cells are extracted by electroporation, though we expect that at a minimum, cytosolic proteins are extracted. We note that since cytosolic enzymes are likely extracted by this process, there are likely kinases that are also extracted, which could potentially counter PTP activity on the substrates by phosphorylating them. However, in another study, we showed that in cell lysates, kinases did not phosphorylate the substrates without the addition of adenosine triphosphate (ATP), a required co-factor for kinase activity.<sup>[35]</sup>

One key feature of the LCAD-SAMDI platform is the ability to study the dynamics of enzymatic activity as demonstrated by the measurement of PTP activity and its changes in response to  $\text{H}_2\text{O}_2$  oxidation in live cells. This indicates that the LCAD-SAMDI method may have potential application in identifying and studying the effects of small molecule inhibitors or drugs, targeting the activity of enzymes that play an important role in disease related pathways. Although we sampled the cells at three different timepoints, it should be possible to extend the process to later timepoints as cell viability is preserved. The number of timepoints at which sampling can be performed is likely limited by cell health in the microfluidic environment and would vary depending on the cell type used.<sup>[36]</sup> Further improvements may be incorporated in the device architecture to improve biocompatibility.<sup>[36]</sup> Another important metric to consider while studying the dynamics of enzymatic activity from live cells is the shortest allowable time gap between two sampling events which determines the temporal resolution of the LCAD-SAMDI system. This is likely limited by the time of recovery of the cells from the initial perturbation such that the second measurement is not biased by the first sampling and does not cause excess cellular damage. A recent study has shown that bulk electroporation may have short and long-term effects on gene expression and cellular function.<sup>[37]</sup> Similar studies on localized electroporation should be pursued to analyze its effect on cells. This will provide an indication of the time gap required between sampling events that minimizes cellular perturbation and measurement bias. Moreover, practical aspects such as the time required for the enzymatic reaction to complete in the sampling chambers (1 h for this study) before a second SAMDI substrate can be introduced, must be considered.



In addition to PTP sampling, we also demonstrated the ability to deliver a protein into cells using the LCAD. Previous studies utilizing localized electroporation have shown that proteins retain their function inside cells post-delivery.<sup>[7]</sup> Moreover our current study shows that PTPs retain their activity on extraction using localized electroporation. This suggests the potential use of the LCAD for efficient delivery of proteins into cells with minimal perturbation to their structure and function, for example, for gene editing studies requiring the delivery of Cas9 ribonucleoproteins (RNPs),<sup>[38]</sup> or for the generation of induced pluripotent stem cells (iPSCs) entailing the delivery of reprogramming proteins such as Oct4 and Sox2.<sup>[39]</sup> Some proteins may require other buffer compositions to maintain proper function, which would require evaluation of compatibility with the LCAD delivery method. Furthermore, localized electroporation has been employed for the intracellular delivery of other exogenous molecules such as siRNA, mRNA and plasmids, in a wide variety of adherent and suspended cell types,<sup>[5–8]</sup> suggesting that the LCAD could be used in studies requiring the delivery of these molecules.<sup>[40–43]</sup> While this work focused on measuring PTP activity, SAMDI is amenable to measuring any enzyme activity that results in a change in mass of the substrate. In addition, localized electroporation has been shown to be effective for extracting other macromolecules, including proteins and nucleic acids in hiPSC derived cardiomyocytes and astrocytes.<sup>[6,9]</sup> Therefore, it may also be possible to duplex measurements to measure both mRNA and enzyme activity simultaneously, enabling a dynamic, genomic and functional proteomic analytical method. With further development, the combined capability of delivery, sampling, and measurement that the LCAD with SAMDI provides could be utilized for mapping external genetic perturbations to the expressed phenotype in different cellular systems. This may find applications in drug screening, cell and tissue engineering, development of cell-based vaccines, disease modelling, and studies involving cell fate.<sup>[44]</sup>

## 4. Conclusion

Methods for evaluating the changes in the activity of enzymes are essential for studying the molecular processes underlying cellular behavior. In this work, we described a method for measuring enzyme activities from living cells that maintained viability and enabled evaluation at multiple time points, before and after treatment. Moreover, the miniaturization achieved by the implementation of microfabrication technology to create multilayered, microfluidic devices, along with the sensitivity of SAMDI, enabled analysis of small numbers of cells, which is a necessity when studying cell samples available in limited quantities. With this unique sampling device and label-free assay format, the LCAD with SAMDI offers a powerful and versatile new method for monitoring the dynamics of cellular activity.

## 5. Experimental Section

**Device Fabrication:** The two molds containing the microchannel and microwell features were prepared using lithography equipment in a clean-room environment. Briefly, a negative photoresist layer (SU-8 2050, Microchem) was spin-coated, UV-exposed, and developed on a

clean Si wafer according to the manufacturer specifications to achieve 50 µm thick features. The mold was then coated with a 500 nm layer of Parylene-C to reduce the surface friction of the mold and facilitate the release of PDMS. The PDMS (Sylgard 184, Dow Corning) elastomer solution was prepared by mixing a 10:1 (w/w) elastomer to curing agent mixture and degassed in a desiccator for 30 min. Through-hole stencils for the microwell layers were fabricated by pouring the PDMS mixture on the mold, covering it with a Mylar sheet (TAP Plastics), and clamping it at 80 °C for 60 min. The Mylar transfer sheet was coated with a Pt-chelating aminosilane, AEAPS (Sigma-Aldrich) that inhibited the polymerization of PDMS between the top of the mold and the surface of the sheet and resulted in through-hole features.<sup>[29]</sup> Two through-hole layers were prepared, one of which was sputter coated with a 100 nm layer of Au. The Au-coated layer was then placed in a  $25 \times 10^{-3}$  M MPTMS (Sigma-Aldrich) in ethanol solution for 180 min and air dried. Simultaneously, the PDMS microchannel layer was prepared by pouring the PDMS mixture on the mold and partially curing in a convection oven at 75 °C for 20 min. Following the MPTMS treatment, the Au-coated microwell layer was aligned with the PDMS microchannels, bonded at 75 °C for 120 min, and placed in room temperature for 12 h. Both PDMS microwell layers were then functionalized with AEAPS in a 1% (v/v) aqueous solution for 20 min. A 25 µm thick PC membrane (Sterlitech) was oxygen plasma treated for 2 min and placed on the AEAPS treated microwell layer. Lastly, the remaining side of the PC membrane was oxygen plasma treated for 2 min, aligned to the bottom microwell layer, and bonded at 110 °C for 120 min.

**Cell Culture:** The tdTomato-expressing MDA-MB 231 cell line was obtained from the developmental therapeutics core (CDT) facility at Northwestern University. The cells were cultured in Dulbecco's modified eagle medium (DMEM) (Gibco) supplemented with 10% Fetal Bovine Serum (FBS) (Gibco) and 1% Penicillin-Streptomycin (Gibco). The cultures were passaged every 3–5 days upon reaching 80–90% confluency using 0.25% Trypsin (Gibco). All experiments were performed on cultures that were passaged less than ten times.

**Cell Seeding:** The fabricated devices were sterilized by placing in 70% ethanol for 15 min and washing with deionized water. The devices were then dried and exposed to UV for 45 min. In order to enhance cell adhesion, the microchannels were flushed with a 1:50 (v/v) solution of 0.1% fibronectin (Sigma Aldrich) in PBS (Gibco) using a syringe pump (New Era). The devices were then incubated overnight at 4 °C to coat the PC membrane surface with fibronectin. The microchannels were then washed with PBS three times to remove unattached residues. The cells were introduced into the microchannel at a density of 7.5 million mL<sup>-1</sup> in DMEM at a flow rate 0.5 µL min<sup>-1</sup>. The flow was then stopped for 10 min during which the cells settled down into the PDMS microwells. Excess cells in the microchannels were removed by washing with DMEM. The devices were then placed in 6-well plates (USA Scientific) and submerged in DMEM. The media could diffuse to the cells through the nanochannels in the PC membrane. The well plates were placed inside an incubator (at 37 °C with 5% CO<sub>2</sub>) for 36 h to allow for cell adhesion and spreading before carrying out the electroporation experiments. DMEM in each well was replenished every 12 h.

**General Electroporation Protocol:** A function generator (Agilent) connected to a voltage amplifier (OPA445, Texas Instruments) was used to apply the electroporation pulses ( $V_1 = 30$  V,  $t_1 = 0.5$  ms;  $V_2 = 10$  V,  $t_2 = 2.5$  ms; 400 pulses at 0.5 Hz). The voltage traces were verified on an oscilloscope (Agilent). The top and bottom ITO-coated glass slides (Nanocs) served as the ground and positive electrodes for pulse application, respectively. The bottom ITO slides used in the enzyme sampling experiments carried the patterned gold spots required for the SAMDI-MS assay. The required buffers were introduced into the top microchannels and the bottom microchambers of the LCAD. Then the LCAD was aligned between the two conductive ITO slides. Once aligned, the assembly was mechanically secured using custom-made clamps. The two electrodes were then connected to the function generator and the desired electroporation pulse train was applied.

**BSA Delivery:** MDA-MB 231 cells expressing tdTomato were seeded and cultured in the LCAD for 24 h. First, the DMEM in the LCAD was replaced with hypo-osmolar electroporation buffer (Eppendorf) by

flowing in the buffer at  $2 \mu\text{L min}^{-1}$  using a syringe pump. Next,  $100 \mu\text{L}$  of Alexa Fluor 488 conjugated BSA solution ( $2.5 \text{ mg mL}^{-1}$  in PBS) was pipetted onto the bottom microchambers of the LCAD. The LCAD was then carefully sandwiched between the two ITO slides, ensuring that there was fluid between the slides and the device for proper electrical contact. Electroporation was carried out using the protocol discussed before, but with the following pulse parameters:  $V_1 = 30 \text{ V}$ ,  $t_1 = 0.5 \text{ ms}$ ;  $V_2 = 10 \text{ V}$ ,  $t_2 = 2.5 \text{ ms}$ ; 200 pulses at  $10 \text{ Hz}$ . After 10 min of incubation at room temperature, the cells were washed by flowing PBS through the microchannels to remove residual BSA. The cells were then imaged for tdTomato expression and positive BSA delivery using fluorescence microscopy. For the control experiments, hypo-osmolar buffer was added to the cell culture wells and fluorescent BSA was loaded underneath the membrane. The devices were incubated for 10 min without the application of the electric pulse. The cells were then washed with PBS and imaged under a fluorescence microscope. The efficiency of BSA delivery was calculated as 
$$\frac{\text{No. of BSA positive cells}}{\text{Total number of cells (from tdTomato expression)}} \times 100\%.$$

**PTP Sampling and Activity Measurement:** MDA-MB 231 expressing tdTomato were seeded and cultured in the LCAD for 36 h before sampling. (Cells used in PTP sampling experiments were not previously used for experiments demonstrating BSA delivery.) Before electroporation, the cells in each microwell were imaged using fluorescence microscopy. The DMEM in the LCAD was then replaced with hypo-osmolar electroporation buffer by flowing in the buffer at  $2 \mu\text{L min}^{-1}$  using a syringe pump. Next,  $100 \mu\text{L}$  of SAMDI buffer ( $20 \times 10^{-3} \text{ M}$  Tris, pH 8,  $136 \times 10^{-3} \text{ M}$  NaCl,  $1 \times 10^{-3} \text{ M}$  EDTA,  $400 \times 10^{-6} \text{ M}$  tris(2-carboxyethyl)phosphine hydrochloride (Sigma), 1 complete mini EDTA-free protease inhibitor cocktail tablet per 10 mL buffer) was pipetted onto the bottom microchambers of the LCAD and the device was sandwiched between the top ITO slide and the bottom SAMDI slide. Then the SAMDI gold spots were aligned to the bottom microchambers of the device under a stereomicroscope. After alignment, electroporation was carried out according to the protocol described above. Following this, the assembly was transferred to the incubator (at  $37^\circ\text{C}$  with  $5\% \text{ CO}_2$ ) to allow for the extracted enzymes to act on the SAMDI substrate. The SAMDI slide was detached and analyzed after 1 h of incubation. Finally, the LCAD was replenished with fresh DMEM, submerged in a 6-well plate filled with DMEM and transferred to the incubator for future analysis. For temporal sampling, the protocol was repeated 24 h after the first electroporation and sampling cycle. When the effect of hydrogen peroxide on PTP activity was evaluated, a baseline measurement of activity was obtained with the electroporation procedure, then the device was incubated an additional 2 h. After this period,  $2 \times 10^{-3} \text{ M}$  hydrogen peroxide in media was loaded into the microchannels for 4 min. The solution was replaced with the hypo-osmolar buffer, and cells were sampled again. The LOD was defined as the mean activity of the control spots (i.e., spots with immobilized substrate but no exposure to cells) +  $3s$ , where  $s$  is the standard deviation of the activity of the control spots. Calculations of activity per cell were made using a lysate standard curve that was fit to a five-parameter logistic equation with MATLAB.

To measure PTP activity from lysates, cells were counted and pelleted in tubes, the supernatant was removed, and lysis buffer was added. Lysis buffer was identical to the SAMDI buffer described above, but with the addition of  $0.1\%$  Triton-X. Dilutions were prepared, and then the lysate was added to monolayers presenting the phospho-peptide substrate and incubated for 1 h,  $37^\circ\text{C}$ . The spots were rinsed with water and ethanol, then analyzed by MALDI MS. Lysate was placed on three spots for each lysate concentration (i.e., three technical replicates). The experiment was performed two times.

**SAMDI Mass Spectrometry:** An electron beam evaporator was used to pattern  $340 \mu\text{m}$  circles of  $5 \text{ nm}$  titanium, and  $30 \text{ nm}$  gold onto ITO-coated glass slides (Nanocs). Monolayers were formed on the gold-patterned slides by incubating the slides overnight at  $4^\circ\text{C}$  in an ethanolic solution of  $0.4 \times 10^{-3} \text{ M}$  alkyl disulfide terminated with tri(ethylene glycol) groups and  $0.1 \times 10^{-3} \text{ M}$  asymmetric disulfide terminated with one tri(ethylene glycol) and one maleimide group. The peptide

CRpY-NH<sub>2</sub>, where pY indicates phosphotyrosine, was immobilized onto the monolayers by incubating a  $40 \times 10^{-6} \text{ M}$  solution of peptide in  $25 \times 10^{-3} \text{ M}$  Tris buffer, pH 8, on the monolayer for 1 h,  $37^\circ\text{C}$ . The slide was then rinsed with water and ethanol, then dried and used as the bottom slide in the LCAD device in the General Electroporation Protocol described above. After the electroporation and incubation, the plate was detached from the device and rinsed with water and ethanol. A  $40 \text{ mg mL}^{-1}$  solution of 2,4,6-trihydroxyacetophenone in acetone was applied and dried over the monolayers on the gold spots. The slides were analyzed with an AB Sciex 5800 MALDI TOF/TOF instrument in positive reflector mode. The area under the curves (AUC) in the mass spectra corresponding to the  $[\text{M}+\text{H}]^+$  and  $[\text{M}+\text{Na}]^+$  disulfide peaks for the substrate and product were analyzed using custom software and average background was subtracted. Activity was defined as:  $\text{AUC}_{\text{Product}} / (\text{AUC}_{\text{Substrate}} + \text{AUC}_{\text{Product}})$ .

**Viability Analysis:** For viability analysis, the cells were stained with Calcein AM (Sigma-Aldrich) and Hoechst 33342 (Life Technologies). A solution of Calcein AM ( $1 \mu\text{g mL}^{-1}$ ) and Hoechst ( $0.1 \text{ mg mL}^{-1}$ ) was prepared in PBS. The solution was introduced into the LCAD microchannels and the device was incubated for 20 min at  $37^\circ\text{C}$ . The microchannels were then washed with PBS and the viability was analyzed using fluorescence microscopy. The cells with Calcein AM and Hoechst fluorescence simultaneously were counted as alive while the ones with only Hoechst were counted as dead.

**Fluorescence Imaging:** Fluorescence images were acquired on a Nikon Eclipse ME 600 Microscope equipped with an Andor Neo sCMOS camera. Image acquisition was controlled using Micro-Manager software.<sup>[45]</sup> The acquired images were analyzed using FIJI, an open source image-processing package.<sup>[46]</sup>

**Statistical Analysis:** Statistical comparisons between mean activities were made using two-tailed Student's *t*-tests.

## Supporting Information

Supporting Information is available from the Wiley Online Library or from the author.

## Acknowledgements

Research reported in this publication was supported by the National Cancer Institute of the National Institutes of Health (NIH) under Award Number U54CA199091 and by NIH R21 Award Number GM132709-01 and the National Institute of General Medical Sciences of the National Institutes of Health under Award Number T32GM105538. This work utilized the Argonne National Lab Center for Nanoscale Materials. Use of the Center for Nanoscale Materials, an Office of Science user facility, was supported by the U.S. Department of Energy, Office of Science, Office of Basic Energy Sciences, under Contract No. DE-AC02-06CH11357. Cells were obtained from the Northwestern University Developmental Therapeutics Core generously supported by NCI CCSG P30 CA060553 awarded to the Robert H Lurie Comprehensive Cancer Center. This work made use of the EPIC facility of Northwestern University's NUANCE Center, which received support from the Soft and Hybrid Nanotechnology Experimental (SHyNE) Resource (NSF ECCS-1542205); the MRSEC program (NSF DMR-1720139) at the Materials Research Center; the International Institute for Nanotechnology (IIN); the Keck Foundation; and the State of Illinois, through the IIN.

## Conflict of Interest

H.D.E. is the founder and majority owner of Infinitesimal LLC, a company commercializing bio-tools for gene editing and cell analysis. M.M. is the founder and chairman of SAMDI Tech Inc., which uses SAMDI-MS to assist clients in the pharmaceutical industry.

## Author Contributions

P.M. and E.J.B. contributed equally to this work. P.M., E.J.B., L.C., J.A.K., M.M., and H.D.E. conceived the project. C.A.P., P.M., E.J.B., and S.S.P.N. designed and fabricated the devices. P.M., E.J.B., C.A.P., E.H.M., L.C., and S.S.P.N. performed the experiments. All authors analyzed and interpreted the data. P.M., E.J.B., C.A.P., M.M., and H.D.E. wrote the manuscript.

## Keywords

cell sampling, electroporation, enzyme activities, microfluidics, nanotechnologies

Received: January 29, 2020

Revised: April 7, 2020

Published online: May 26, 2020

- [1] A. Ostman, C. Hellberg, F. D. Bohmer, *Nat. Rev. Cancer* **2006**, 6, 307.
- [2] D. P. Labbe, S. Hardy, M. L. Tremblay, *Prog. Mol. Biol. Transl. Sci.* **2012**, 106, 253.
- [3] P. Actis, M. M. Maalouf, H. J. Kim, A. Lohith, B. Vilozny, R. A. Seger, N. Pourmand, *ACS Nano* **2014**, 8, 546.
- [4] O. Guillaume-Gentil, R. V. Grindberg, R. Kooger, L. Dorwling-Carter, V. Martinez, D. Ossola, M. Pilhofer, T. Zambelli, J. A. Vorholt, *Cell* **2016**, 166, 506.
- [5] W. Kang, J. P. Giraldo-Vela, S. S. P. Nathamgari, T. McGuire, R. L. McNaughton, J. A. Kessler, H. D. Espinosa, *Lab Chip* **2014**, 14, 4486.
- [6] P. Mukherjee, S. S. P. Nathamgari, J. A. Kessler, H. D. Espinosa, *ACS Nano* **2018**, 12, 12118.
- [7] Y. Cao, E. Ma, S. Cestellos-Blanco, B. Zhang, R. Qiu, Y. Su, J. A. Doudna, P. Yang, *Proc. Natl. Acad. Sci. USA* **2019**, 116, 7899.
- [8] S. S. P. Nathamgari, P. Mukherjee, J. A. Kessler, H. D. Espinosa, *Proc. Natl. Acad. Sci. USA* **2019**, 116, 22909.
- [9] Y. Cao, M. Hjort, H. Chen, F. Birey, S. A. Leal-Ortiz, C. M. Han, J. G. Santiago, S. P. Pasca, J. C. Wu, N. A. Melosh, *Proc. Natl. Acad. Sci. USA* **2017**, 114, E1866.
- [10] M. Mrksich, *ACS Nano* **2008**, 2, 7.
- [11] T. Kotnik, W. Frey, M. Sack, S. Haberl Meglič, M. Peterka, D. Miklavčič, *Trends Biotechnol.* **2015**, 33, 480.
- [12] M. L. Yarmush, A. Golberg, G. Serša, T. Kotnik, D. Miklavčič, *Annu. Rev. Biomed. Eng.* **2014**, 16, 295.
- [13] W. Kang, F. Yavari, M. Minary-Jolandan, J. P. Giraldo-Vela, A. Safi, R. L. McNaughton, V. Parpoil, H. D. Espinosa, *Nano Lett.* **2013**, 13, 2448.
- [14] P. E. Boukany, A. Morss, W. C. Liao, B. Henslee, H. Jung, X. Zhang, B. Yu, X. Wang, Y. Wu, L. Li, K. Gao, X. Hu, X. Zhao, O. Hemminger, W. Lu, G. P. Lafyatis, L. J. Lee, *Nat. Nanotechnol.* **2011**, 6, 747.
- [15] Y. Cao, H. Chen, R. Qiu, M. Hanna, E. Ma, M. Hjort, A. Zhang, R. S. Lewis, J. C. Wu, N. A. Melosh, *Sci. Adv.* **2018**, 4, eaat8131.
- [16] R. Yang, V. Lemaître, C. Huang, A. Haddadi, R. McNaughton, H. D. Espinosa, *Small* **2018**, 14, 1702495.
- [17] W. Kang, R. L. McNaughton, H. D. Espinosa, *Trends Biotechnol.* **2016**, 34, 665.
- [18] L. Chang, L. Li, J. Shi, Y. Sheng, W. Lu, D. Gallego-Perez, L. J. Lee, *Lab Chip* **2016**, 16, 4047.
- [19] G. He, C. Yang, T. Hang, D. Liu, H. J. Chen, A. H. Zhang, D. Lin, J. Wu, B. R. Yang, X. Xie, *ACS Sens.* **2018**, 3, 1675.
- [20] J. Su, M. Mrksich, *Angew. Chem., Int. Ed.* **2002**, 41, 4715.
- [21] H. D. Min, J. Su, M. Mrksich, *Angew. Chem., Int. Ed.* **2004**, 43, 5973.
- [22] L. C. Szymczak, C. F. Huang, E. J. Berns, M. Mrksich, *Methods Enzymol.* **2018**, 607, 389.
- [23] Z. A. Gurard-Levin, K. A. Kilian, J. Kim, K. Bähr, M. Mrksich, *ACS Chem. Biol.* **2010**, 5, 863.
- [24] L. Ban, N. Pettit, L. Li, A. D. Stuparu, L. Cai, W. Chen, W. Guan, W. Han, P. G. Wang, M. Mrksich, *Nat. Chem. Biol.* **2012**, 8, 769.
- [25] J. Su, T. W. Rajapaksha, M. E. Peter, M. Mrksich, *Anal. Chem.* **2006**, 78, 4945.
- [26] S. E. Wood, G. Sinsinbar, S. Gudlur, M. Nallani, C. F. Huang, B. Liedberg, M. Mrksich, *Angew. Chem., Int. Ed.* **2017**, 56, 16531.
- [27] C. L. Crespi, D. M. Stresser, *J. Pharmacol. Toxicol. Methods* **2000**, 44, 325.
- [28] M. C. Maillard, C. Dominguez, M. J. Gemkow, F. Krieger, H. Park, S. Schaertl, D. Winkler, I. Muñoz-Sanjuán, **2013**, 18, 868.
- [29] J. M. Karlsson, T. Haraldsson, C. F. Carlborg, J. Hansson, A. Russom, W. Van Der Wijngaart, *J. Micromech. Microeng.* **2012**, 22, 085009.
- [30] M. P. Stewart, R. Langer, K. F. Jensen, *Chem. Rev.* **2018**, 118, 7409.
- [31] T. C. Meng, T. Fukada, N. K. Tonks, *Mol. Cell* **2002**, 9, 387.
- [32] A. Östman, J. Frijhoff, A. Sandin, F. D. Böhmer, *J. Biochem.* **2011**, 150, 345.
- [33] N. Krishnan, C. A. Bonham, I. A. Rus, O. K. Shrestha, C. M. Gauss, A. Haque, A. Tocilj, L. Joshua-Tor, N. K. Tonks, *Nat. Commun.* **2018**, 9, 283.
- [34] A. Alonso, J. Sasin, N. Bottini, I. Friedberg, I. Friedberg, A. Osterman, A. Godzik, T. Hunter, J. Dixon, T. Mustelin, *Cell* **2004**, 117, 699.
- [35] L. C. Szymczak, D. J. Sykora, M. Mrksich, *Chem. - Eur. J.* **2020**, 26, 165.
- [36] S. Halldorsson, E. Lucumi, R. Gómez-Sjöberg, R. M. T. Fleming, *Biosens. Bioelectron.* **2015**, 63, 218.
- [37] T. DiTommaso, J. M. Cole, L. Cassereau, J. A. Buggé, J. L. S. Hanson, D. T. Bridgen, B. D. Stokes, S. M. Loughhead, B. A. Beutel, J. B. Gilbert, K. Nussbaum, A. Sorrentino, J. Toggweiler, T. Schmidt, G. Gyulveszti, H. Bernstein, A. Sharei, *Proc. Natl. Acad. Sci. USA* **2018**, 115, E10907.
- [38] S. Kim, D. Kim, S. W. Cho, J. Kim, J. S. Kim, *Genome Res.* **2014**, 24, 1012.
- [39] D. Kim, C. H. Kim, J. I. Moon, Y. G. Chung, M. Y. Chang, B. S. Han, S. Ko, E. Yang, K. Y. Cha, R. Lanza, K. S. Kim, *Cell Stem Cell* **2009**, 4, 472.
- [40] A. Wittrup, J. Lieberman, *Nat. Rev. Genet.* **2015**, 16, 543.
- [41] T. L. Roth, C. Puig-Saus, R. Yu, E. Shifrut, J. Carnevale, P. J. Li, J. Hiatt, J. Saco, P. Krystofinski, H. Li, V. Tobin, D. N. Nguyen, M. R. Lee, A. L. Putnam, A. L. Ferris, J. W. Chen, J. N. Schickel, L. Pellerin, D. Carmody, G. Alkorta-Aranburu, D. Del Gaudio, H. Matsumoto, M. Morell, Y. Mao, M. Cho, R. M. Quadros, C. B. Gurumurthy, B. Smith, M. Haugwitz, S. H. Hughes, J. S. Weissman, K. Schumann, J. H. Esensten, A. P. May, A. Ashworth, G. M. Kupfer, S. A. W. Greeley, R. Bacchetta, E. Meffre, M. G. Roncarolo, N. Romberg, K. C. Herold, A. Ribas, M. D. Leonetti, A. Marson, *Nature* **2018**, 559, 405.
- [42] J. Liu, T. Gaj, Y. Yang, N. Wang, S. Shui, S. Kim, C. N. Kanchiswamy, J. S. Kim, C. F. Barbas III, *Nat. Protoc.* **2015**, 10, 1842.
- [43] S. E. Howden, J. A. Thomson, M. H. Little, *Nat. Protoc.* **2018**, 13, 875.
- [44] M. P. Stewart, A. Sharei, X. Ding, G. Sahay, R. Langer, K. F. Jensen, *Nature* **2016**, 538, 183.
- [45] A. D. Edelstein, M. A. Tsuchida, N. Amodaj, H. Pinkard, R. D. Vale, N. Stuurman, *J. Biol. Methods* **2014**, 1, 10.
- [46] J. Schindelin, I. Arganda-Carreras, E. Frise, V. Kaynig, M. Longair, T. Pietzsch, S. Preibisch, C. Rueden, S. Saalfeld, B. Schmid, J. Y. Tinevez, D. J. White, V. Hartenstein, K. Eliceiri, P. Tomancak, A. Cardona, *Nat. Methods* **2012**, 9, 676.